Journal of Engineering Science and Technology Review 18 (2) (2025) 120- 124

Research Article

JOURNAL OF
Engineering Science and Technology Review

www.jestr.org

Heat Transfer Performance of Supercritical Methane for Liquid Rocket Engines

Djeffal Mohammed Amine*, Nabila Alili, Abdelkader Lahcene, Ali Benouar, Nabil Benamara, Khacem Kaddouri, Mokadem Salem and Abdelkader Boulenouar

Mechanical Engineering Department, Djillali Liabes University, Laboratory of materials and Reactive Systems (LMSR), Sidi Bel Abbes, Algeria.

Received 18 December 2024; Accepted 4 March 2025

Abstract

This study investigates the heat transfer performance of supercritical methane in regenerative cooling channels for liquid-propellant rocket engines. The research focuses on comparing two channel geometries: circular and square, under varying heat fluxes and inlet velocities, as well as examining the effect of channel surface area on heat transfer and pressure losses. Results indicate that the square channel outperforms the circular channel in heat transfer efficiency, particularly at high heat fluxes and low velocities. The phenomenon of heat transfer deterioration, observed in the circular channel at low velocities and high heat fluxes, is eliminated in the square channel, highlighting its superior thermal performance. However, the square channel incurs higher pressure losses. Finally, increasing the channel surface area significantly enhances heat transfer, mitigates heat transfer deterioration, and reduces pressure losses. These findings highlight the critical role of optimizing channel geometry, surface area, and flow parameters to enhance regenerative cooling systems' performance.

Keywords: Regenerative cooling, Supercritical methane, Square and circular channels, Liquid-propellant rocket engines,s Heat transfer deterioration.

1. Introduction

There are three types of chemical rocket engines: liquid propellant, solid propellant, and hybrid. The distinction between these types is primarily based on the physical state of the propellant pair, i.e., the oxidizer and the fuel. Among these three categories, liquid propulsion stands out due to its numerous advantages, including high specific impulse and the ability to modulate thrust. These characteristics make it a preferred choice for space launch vehicles and long-range or intercontinental ballistic missiles.

In recent years, significant research efforts have been dedicated to developing next-generation rocket engines. These studies focus on various aspects such as design, manufacturing, ignition, combustion, and more [1-7]. Due to the extremely high temperatures generated by combustion gases, rocket engines require efficient cooling systems. Consequently, many recent studies have explored innovative cooling methods to further improve their efficiency [8-15].

Each type of propulsion has its own cooling system. As illustrated in Fig. 1, regenerative cooling is indispensable for applications requiring high pressures, forces, and long combustion durations. This cooling method is particularly well-suited to liquid propulsion [16, 17].

The principle of regenerative cooling involves surrounding the engine with a series of channels through which the fuel typically flows before being injected into the combustion chamber. This fuel absorbs part of the heat, helping to maintain the engine's temperature within acceptable limits.

The choice of fuel for liquid-propellant rocket engines also depends on several criteria, such as its density, cost, the ability to be synthesized on other planets like Mars etc. Over the past decade, methane has emerged as a promising candidate for next-generation rocket engines. It offers an excellent balance between density, cost, and thermophysical properties, presenting a good compromise of advantages compared to kerosene and hydrogen in several areas [18, 19].

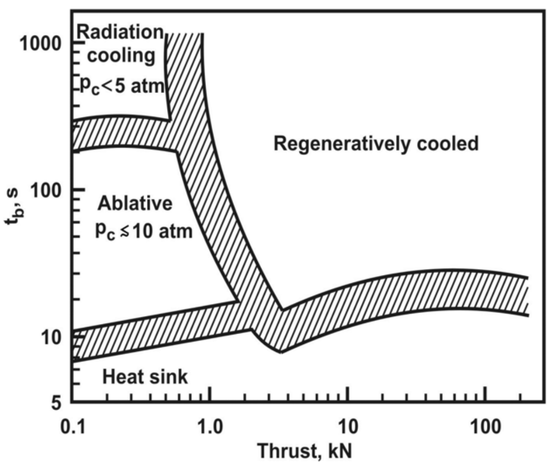

Fig. 1. Regimes for using different cooling techniques [16].

In regenerative cooling systems, methane enters the cooling channels at a pressure above its critical pressure. As its temperature rises, it does not undergo a phase transition but reaches a so-called "pseudo-critical" temperature, where its thermophysical properties change significantly. Near this temperature, the specific heat reaches a maximum, while density, thermal conductivity, and viscosity decrease considerably. Moreover, high operating pressure reduces variations in these properties as shown in Fig. 2 which

*E-mail address: djeffalmohammed66@gmail.com
ISSN: 1791-2377
doi:10.25103/jestr.182.15

presents NIST data depicting the variation of methane's specific heat and density across a range of supercritical pressures and temperatures [20].

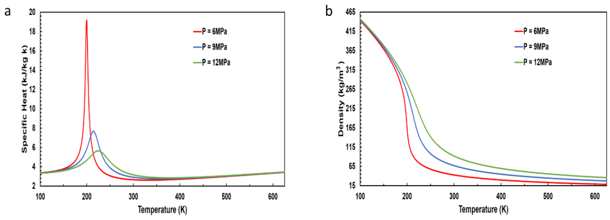

Fig. 2. Specific heat (a) and density (b), of Methane at different temperatures supercritical pressures [20].

This work aims to study the heat transfer of supercritical methane by comparing two types of channels: circular and square. The investigations focus on different boundary conditions, as well as the effect of channel surface modifications on heat transfer and pressure losses.

2. Modelling and simulation

The aim of our research is to study the influence of heat flux and methane inlet velocity on forced convection heat transfer by comparing two channel configurations: circular and square, both having a constant cross-sectional area of 9 mm². Each channel has a length of 300 mm, which is typically equivalent to the length of a combustion chamber, and is heated on its lower surface, as illustrated in Fig. 3. To ensure a fully developed flow at the inlet and to avoid boundary condition effects at the outlet, two fluid sections of 150 mm length were added to both ends of the channel. Due to symmetry, only half of the channel, along the *z*-plane, is modeled in the numerical calculations.

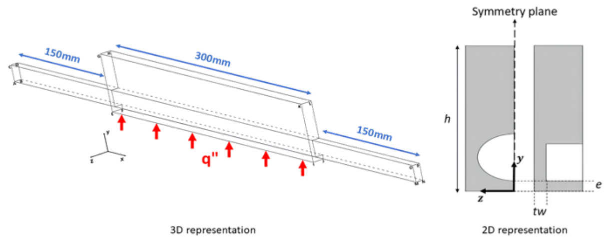

Fig. 3. Solution domain.

To investigate the effect of cross-sectional area on heat transfer and pressure losses, we will compare not only the circular and square channels with a cross-sectional area of 9 mm² but also other channels with areas of 4 mm² and 16 mm².

The material used for this research is a copper alloy, which is commonly employed in liquid-propellant rocket engines. The total channel height h is 14 mm, with a fixed inner wall thickness e of 1 mm. The width of the square channel is dimensioned so that the rib base t_w is 1 mm, regardless of the channel's cross-sectional area.

The boundary conditions shown in Table 1 include an inlet temperature T_i of 120 K and an outlet pressure P_e of 9 MPa for all channels. To analyze the effect of heat flux and inlet velocity on heat transfer, the channels will be exposed to heat fluxes q'' of 2, 4, and 6 MW/m² on their lower surface. The inlet velocities u_∞ considered are 10, 15, and 20 m/s.

For the study of the effect of cross-sectional area, only extreme conditions — the lowest inlet velocity (10 m/s) and the highest heat flux (6 MW/m²) — will be tested.

The thermophysical properties of methane were extracted from the NIST database [20], while the variation of the thermal conductivity λ of copper follows the data from Simon et al [21].

Table 1. Boundary conditions.

Plans	Conditions
GHKL	$\frac{\partial T}{\partial n} = 0$
EFIJ	$\frac{\partial T}{\partial n} = q''$
CDOP	$\frac{\partial T}{\partial n} = 0$
ABMN	$\frac{\partial T}{\partial n} = 0$
EFGH	$\frac{\partial T}{\partial n} = 0$
IJKL	$\frac{\partial T}{\partial n} = 0$
ABCD	T_i, u_∞
MNOP	P_e
FHJL, BDNP	Plans de symétrie

The 3D numerical simulations were carried out using ANSYS Fluent 18.1. The fluid flow and heat transfer within the cooling channels were assumed to be steady and turbulent. A tetrahedral mesh was applied to the entire domain (solid and fluid), with the boundary layer near the walls refined using the Inflation option in the meshing tool. The k−ε turbulence model with enhanced wall treatment was chosen for its ability to accurately capture steep temperature gradients near the walls while maintaining y+ ≤ 1 across all fluid-solid interfaces. This model is widely adopted in this type of study due to its balance between accuracy and computational efficiency, providing results that closely match reality compared to models like k-ω SST and RNG k-ε. Although the Reynolds Stress Model offers greater precision in certain cases, it demands significantly higher computational resources, time, and storage capacity, making the k−ε model a more practical choice.

3. Grid convergence

To ensure mesh-independent results and minimize computational time, a convergence study of the maximum heated wall temperature T_{wg} versus heat flux for the circular channel with a heat flux of 6 MW/m² and an inlet velocity of 10 m/s was conducted for various element sizes.

As shown in Fig. 4, it was observed that mesh convergence was achieved starting from an element size of 4×10^-04m. This element size was therefore adopted for all subsequent simulations.

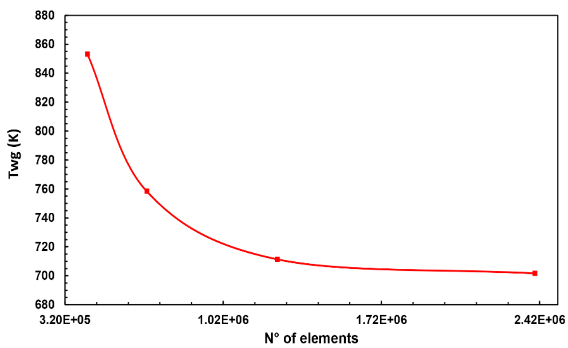

Fig. 4. Convergence of the maximum heated wall temperature.

4. Model Validation

The model validation was performed using the experimental study of Hongfang Gu et al. In their study, they investigated convective heat transfer from a horizontal miniature tube to methane at supercritical pressures under different pressures, mass velocities, and heat fluxes. They used a stainless-steel miniature circular tube with a heating length of 200 mm, a diameter of 2.6 mm, and a wall thickness of 0.5 mm. The outlet pressure was set to 10 MPa. For this validation, we fixed the heat flux q" at 6.5 MW/m² and the mass velocity at 7000 kg/m²s, and we analyzed the evolution of the wall temperature tw relative to the pseudo-critical temperature, as a function of the bulk temperature tb relative to the pseudo-critical temperature. The results obtained, presented in Fig. 5, show good agreement between the present study and the findings of Hongfang Gu et al.

5. Results and Discussions

5.1 Heat Transfer Difference Between Circular and Square Channels

The comparison between the two channels shows that the square channel outperforms the circular channel in terms of heat transfer efficiency. This difference becomes increasingly apparent at higher heat fluxes and lower velocities. For example, at a velocity of 10 m/s and a heat flux of 6 MW/m², the heated wall temperature T_{wg} difference between the two channels reached approximately 165.4K, and approximately 145.9K for the adiabatic wall temperature T_{wa} which is very significant. This temperature difference can be attributed to the geometry of the two channels and the way temperature is distributed.

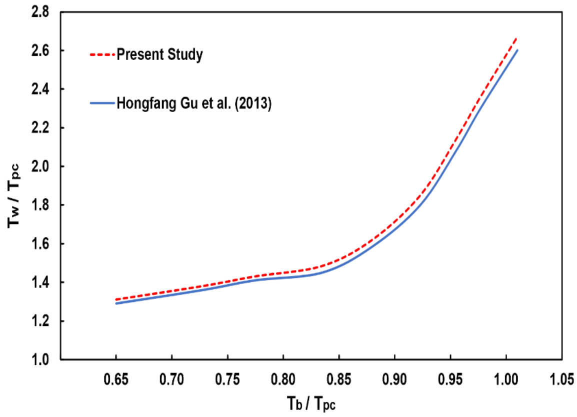

Fig. 5. Comparison of the Present Study with Experimental Findings of Hongfang Gu et al.

However, the disadvantage of the square channel compared to the circular one is that it causes higher pressure losses because of its shape and especially its edges which generate more turbulence and therefore more pressure losses. These differences are clear regardless of the boundary conditions as shown in the accompanying tables 2, 3 and 4.

Table 2. Maximum wall temperatures T_{wg} and T_{wa}, and pressure losses at an inlet velocity u_{∞}= 10m/s and different heat fluxes q''.

	2MW/m²		4MW/m²		6MW/m²	
	Square	Circular	Square	Circular	Square	Circular
Twg Max (K)	205.53	211.94	322.37	341.15	528.16	665.62
Twa Max (K)	176.46	184.13	262.40	284.60	427.93	573.71
dP (MPa)	0.033	0.028	0.029	0.027	0.037	0.035

Table 3. Maximum wall temperatures T_{wg} and T_{wa}, and pressure losses at an inlet velocity u_{∞}= 15m/s and different heat fluxes q''.

	2MW/m²		4MW/m²		6MW/m²	
	Square	Circular	Square	Circular	Square	Circular
Twg Max (K)	183.45	187.81	262.64	274.70	354.72	375.11
Twa Max (K)	155.94	161.28	204.91	220.01	266.36	291.21
dP (MPa)	0.068	0.059	0.063	0.056	0.060	0.058

Table 4. Maximum wall temperatures T_{wg} and T_{wa}, and pressure losses at an inlet velocity u_{∞}= 20m/s and different heat fluxes q''.

	2MW/m²		4MW/m²		6MW/m²	
	Square	Circular	Square	Circular	Square	Circular
Twg Max (K)	172.45	175.27	232.16	239.51	301.47	315.59
Twa Max (K)	146.44	150.03	177.64	186.79	218.78	236.18
dP (MPa)	0.1126	0.098	0.1104	0.099	0.1018	0.094

Another notable observation as shown in Fig. 6, is that at low velocities and high heat fluxes, the circular channel exhibits the phenomenon of heat transfer deterioration. This is characterized by a sudden wall temperature rise from 440.4 K at 0.1 m from the inlet to 651.8 K at 0.25 m, indicating a drastic increase of 211.4 K over a mere 0.15 m. This phenomenon occurs when the wall temperature near the channel reaches the pseudo-critical temperature, while the bulk temperature remains lower, leading to a separation between these two regions, as shown in previous studies [10, 14].

In contrast, this heat transfer deterioration was not observed in the square channel. This emphasizes how the choice of channel geometry plays a critical role in determining the quality of heat transfer.

Increasing the inlet velocity to enhance heat transfer and eliminate the occurrence of heat transfer deterioration is a feasible solution. However, it is essential to account for the rise in pressure losses. For instance, a 241.2% increase in pressure losses was observed in the square channel for a heat flux of 2 MW/m² when the velocity increased from 10 to 20 m/s. This increase is significant, especially considering that we are only working with a channel size equivalent to that of a combustion chamber. This indicates that the losses would be even greater if the full geometry and length of a rocket engine nozzle were considered.

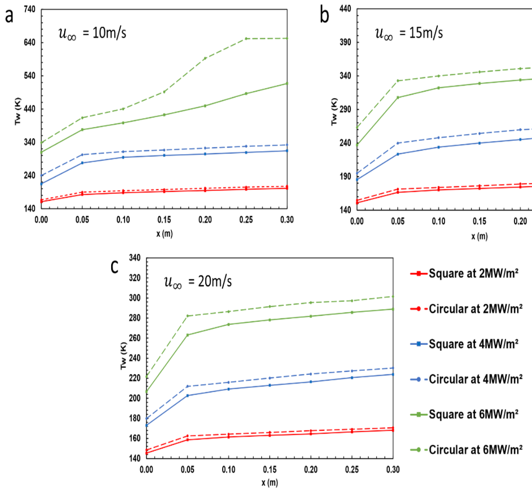

Fig. 6. Liquid side wall temperatures T_w at different positions.

5.2 The Effect of Varying Channel Surface Area

Fig. 7, Fig. 8 and table 5 show that increasing the channel's surface area significantly enhances heat transfer. For instance, in the circular channel, a reduction of 88.4 K in temperature was observed when increasing the surface area from 4 mm² to 16 mm². Additionally, there is a notable attenuation of the heat transfer deterioration phenomenon as the surface area increases. This phenomenon, present in both channels with a surface area of 4 mm² and only in the circular channel with a surface area of 9 mm², was no longer observed with a surface area of 16 mm².

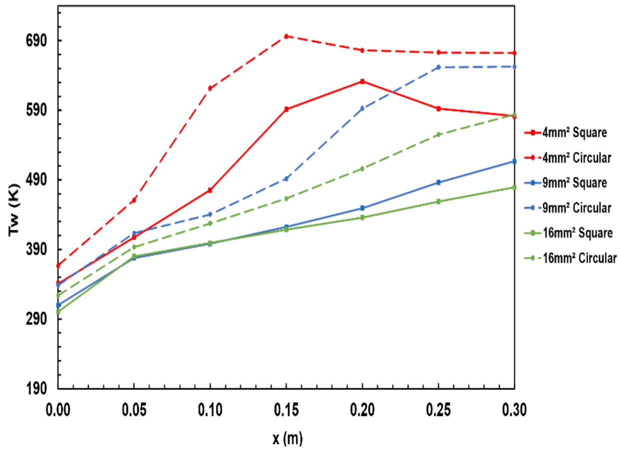

Fig. 7. Liquid side wall temperatures T_w at different positions for different channel surfaces.

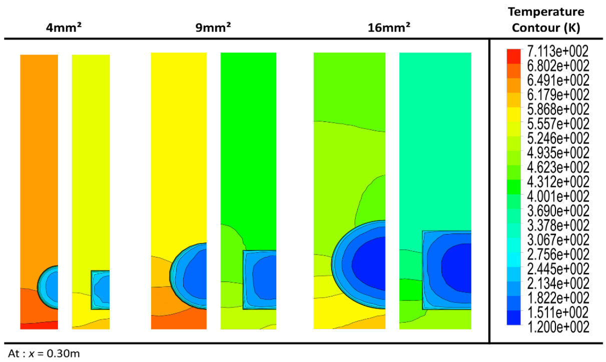

Fig. 8. Temperature contours of the two channels for different surfaces at the outlet.

Table 5. Maximum wall temperatures T_{wg} and T_{wa}, and pressure losses at an inlet velocity u_∞= 10m/s and a heat fluxes q'' = 6MW/m².

	4mm		9mm		16mm	
	Square	**Circular**	**Square**	**Circular**	**Square**	**Circular**
Twg Max (K)	644.23	711.28	528.16	665.62	490.53	595.99
Twa Max (K)	581.98	652.74	427.93	573.71	345.01	462.04
dP (MPa)	0.075	0.074	0.037	0.035	0.024	0.022

Moreover, the increase in surface area substantially reduced pressure losses. For example, in the case of the square channel, pressure losses decreased by 215.5% when the surface area increased from 4 mm² to 16 mm².

Therefore, the selection and sizing of the channel surface area have a significant impact on heat transfer quality and pressure losses. These parameters must be carefully analyzed and optimized during the design of cooling systems.

6. Conclusion

Through these three-dimensional numerical simulations on the heat transfer of supercritical methane in regenerative cooling channels for liquid propellant rocket engines, comparing the performance of two channel geometries (circular and square) at various heat fluxes and velocities, while also investigating the effect of channel surface size on heat transfer and pressure losses, the following conclusions can be drawn:

- The square channel exhibits better heat transfer performance compared to the circular channel. This difference becomes increasingly noticeable at high heat fluxes and low velocities. However, the square channel also generates higher pressure losses compared to the circular channel, because of its shape and especially its edges which generate more turbulence and therefore more pressure losses.
- The square channel eliminates the occurrence of the heat transfer deterioration phenomenon, which was observed in the circular channel at low velocities and high heat fluxes. This highlights a significant advantage of the square geometry compared to the circular one.
- High thermal fluxes require high inlet velocities to ensure efficient heat transfer and prevent thermal deterioration. However, the associated increase in pressure losses must be carefully considered.
- Increasing the channel surface area improves heat transfer, mitigates heat transfer deterioration, and even reduces pressure losses.

In summary, this study demonstrates that supercritical heat transfer in regenerative cooling systems for liquid-propellant rocket engines can be optimized by selecting appropriate channel geometry and size, and by adjusting flow parameters.

References

[1] N. Alili, K. Kaddouri, S. Mokadem, and A. Alami, "Numerical Analysis of Convergent-Divergent Angles and Operating Conditions Impact on Rocket Nozzle Performance Parameters," *INCAS Bull.*, vol. 16, pp. 3–14, Mar. 2024, doi: 10.13111/2066-8201.2024.16.1.1.

[2] N. Alili, A. Benouar, M. A. Djeffal, K. Kaddouri, and M. Salem, "Novel Circular Arc Contour Design for Optimizing Rocket Nozzle Efficiency," *J. Aeron., Astron. Aviaτ.*, vol. 56, no. 4, pp. 801–809, Sep. 2024, doi: 10.6125/JoAAA.202409_56(4).02

[3] D. S. Scannapieco, J. J. Lewandowski, R. B. Rogers, and D. L. Ellis, "In-Situ Alloying of GRCop-42 via Additive Manufacturing: Precipitate Analysis," Technical Memorandum E-19858, Aug. 2020. [Online]. Available: https://ntrs.nasa.gov/citations/20205003857

[4] P. R. Gradl *et al.*, "Lightweight Thrust Chamber Assemblies using Multi-Alloy Additive Manufacturing and Composite Overwrap," in *AIAA Propuls. Ener. 2020 Forum*, Virtual Event: American Institute of Aeronautics and Astronautics, Aug. 2020. doi: 10.2514/6.2020-3787.

[5] N. Kabbe, A. Lohar, A. Panchaxarimath, and V. Tiwary, "Revolutionizing Aerospace Industries through Additive Manufacturing: Innovations, Challenges, and Prospects," *J. Aeron., Astronaut. Aviat.*, vol. 56, no. 2, pp. 593–602, Sep. 2024. doi:10.6125/JoAAA.202406_56(2).07

[6] S. A. O'Briant, S. B. Gupta, and S. S. Vasu, "Review: laser ignition for aerospace propulsion," *Propuls. Power Res.*, vol. 5, no. 1, pp. 1–21, Mar. 2016, doi: 10.1016/j.jppr.2016.01.004.

[7] T. Mundt, C. Knowlen, and M. Kurosaka, "Scale effects on rotating detonation rocket engine operation," *Applicat. Energy Combust. Sci.*, vol. 19, Sep. 2024, Art. no. 100282, doi: 10.1016/j.jaecs.2024.100282.

[8] M. A. Djeffal, N. Benamara, A. Lahcene, A. Benouar, A. Boulenouar, and M. Merzoug, "Numerical Analysis of a Supercritical Heat Transfer of Cryogenic Methane in Regeneratively Cooled Rocket Engine," *INCAS Bull*, vol. 16, no. 1, pp. 33–44, Mar. 2024, doi: 10.13111/2066-8201.2024.16.1.4.

[9] Mohammed Amine Djeffal *et al.*, "Numerical Analysis of Supercritical Methane Heat Transfer in Regeneratively Cooled Liquid Propellant Rocket Engines," *J. Aeronaut., Astronaut. Aviat.*, vol. 56, no. 4, pp. 835-844, Sep. 2024, doi: 10.6125/JoAAA.202409_56(4).05.

[10] M. Leonardi, M. Pizzarelli, and F. Nasuti, "Analysis of thermal stratification impact on the design of cooling channels for liquid rocket engines," *Int. J. Heat Mass Transf.*, vol. 135, pp. 811–821, Jun. 2019, doi: 10.1016/j.ijheatmasstransfer.2019.02.028.

[11] F. Nasuti and M. Pizzarelli, "Pseudo-boiling and heat transfer deterioration while heating supercritical liquid rocket engine propellants," *The J. Supercrit. Fluids*, vol. 168, Feb. 2021, Art. no. 105066, doi: 10.1016/j.supflu.2020.105066.

[12] M. Pizzarelli and F. Battista, "Oxygen–methane rocket thrust chambers: Review of heat transfer experimental studies," *Acta Astronaut.*, vol. 209, pp. 48–66, Aug. 2023, doi: 10.1016/j.actaastro.2023.04.028.

[13] A. Ulas and E. Boysan, "Numerical analysis of regenerative cooling in liquid propellant rocket engines," *Aerosp. Sci. Techn.*, vol. 24, no. 1, pp. 187–197, Jan. 2013, doi: 10.1016/j.ast.2011.11.006.

[14] H. Gu, H. Li, H. Wang, and Y. Luo, "Experimental investigation on convective heat transfer from a horizontal miniature tube to methane at supercritical pressures," *Appl. Thermal Eng.*, vol. 58, no. 1–2, pp. 490–498, Sep. 2013, doi: 10.1016/j.applthermaleng.2013.04.049.

[15] J. Haemisch, D. Suslov, and M. Oschwald, "Experimental Study of Methane Heat Transfer Deterioration in a Subscale Combustion Chamber," *J. Propuls. Power*, vol. 35, no. 4, pp. 819–826, Jul. 2019, doi: 10.2514/1.B37394.

[16] H. S. Mukunda, *Understanding aerospace chemical propulsion*. New Delhi: I.K. International Pub. House, 2017.

[17] G. P. Sutton and O. Biblarz, *Rocket propulsion elements*, Ninth edition. Hoboken, New Jersey: John Wiley & Sons Inc, 2017.

[18] H. Trinh, "Liquid methane/oxygen injector study for potential future Mars ascent," in *36th AIAA/ASME/SAE/ASEE Joint Propuls. Conf. Exhib.*, Las Vegas,NV, U.S.A.: American Institute of Aeronautics and Astronautics, Jul. 2000. doi: 10.2514/6.2000-3119.

[19] T. Brown, M. Klem, and P. McRight, "Foundational Methane Propulsion Related Technology Efforts, and Challenges for Applications to Human Exploration Beyond Earth Orbit," Marshall Space Flight Center, Rome, Italy, M16-5248, May 2016. [Online]. Available: https://ntrs.nasa.gov/citations/20160006972

[20] E. W. Lemmon, I. H. Bell, M. L. Huber, and M. O. McLinden, Thermophysical Properties of Fluid Systems. National Institute of Standards and Technology, 2023. https://webbook.nist.gov/chemistry/fluid/

[21] N. Simon, E. Drexler, and R. Reed, "Properties of copper and copper alloys at cryogenic temperatures. Final report," PB-92-172766/XAB, NIST/MONO--177, 5340308, Feb. 1992. doi: 10.2172/5340308.